

Liquid lithium surface control and its effect on plasma performance in the HT-7 tokamak



G.Z. Zuo^a, J. Ren^a, J.S. Hu^{a,*}, Z. Sun^a, Q.X. Yang^a, J.G. Li^a, L.E. Zakharov^b, David N. Ruzic^c, the HT-7 team

^a Institute of Plasma Physics, Chinese Academy of Sciences, Hefei 230031, China

^b Princeton University Plasma Physics Laboratory Princeton, NJ 08543, USA

^c University of Illinois, Urbana, IL 61801, USA

HIGHLIGHTS

- Strong interaction between plasma and Li would cause strong Li emission and lead to disruptive plasmas, and probable reasons were analyzed.
- Serious Li would be emitted from the free statics surface mainly due to $J \times B$ force leading to plasma instable and disruptions.
- CPS surface would partially suppress the emission and be beneficial for plasma operation.
- Li emission from flowing LLLs on free surfaces on SS trenches and on SS plate were compared.

ARTICLE INFO

Article history:

Received 29 November 2013
Received in revised form 21 May 2014
Accepted 21 May 2014
Available online 14 June 2014

Keywords:

Liquid lithium limiter
CPS
Li efflux
Disruptions
HT-7

ABSTRACT

Experiments with liquid lithium limiters (LLLs) have been successfully performed in HT-7 since 2009 and the effects of different limiter surface structures on the ejection of Li droplets have been studied and compared. The experiments have demonstrated that strong interaction between the plasma and the liquid surface can cause intense Li efflux in the form of ejected Li droplets – which can, in turn, lead to plasma disruptions. The details of the LLL plasma-facing surface were observed to be extremely important in determining performance. Five different LLLs were evaluated in this work: two types of static free-surface limiters and three types of flowing liquid Li (FLLL) structures. It has been demonstrated that a FLLL with a slowly flowing thin liquid Li film on vertical flow plate which was pre-treated with evaporated Li was much less susceptible to Li droplet ejection than any of the other structures tested in this work. It was further observed that the plasmas run against this type of limiter were reproducibly well-behaved. These results provide technical references for the design of FLLLs in future tokamaks so as to avoid strong Li ejection and to decrease disruptive plasmas.

© 2014 Elsevier B.V. All rights reserved.

1. Introduction

In a future fusion research device a liquid lithium (Li) wall which flowed continuously could effectively reduce hydrogenic recycling and suppress impurity influx from plasma-facing materials (PFMs). Such a system could also continuously remove the high heat flux resulting from the impingement of high-energy plasma particles while simultaneously regenerating damaged surfaces [1,2]. These possibilities have motivated experiments on the HT-7 fusion device described in this work.

Experiments with liquid Li limiters (LLLs) have previously been carried out in tokamaks for the enhancement of plasma performance. Some successes and some difficulties have been encountered in those efforts. For example in CDX-U [3–6] plasma discharges with lower wall recycling, lower edge impurity radiation and higher core electron temperatures were obtained by using a static toroidal LLL. Excellent results were also achieved in both FTU and T-11M by application of LLLs in the form of the capillary-porous system (CPS) [7–11]. However, experiments on CDX-U using a horizontal CPS located at the top of the plasma column demonstrated that macroscopic Li droplets tended to fall (or be ejected) toward the plasma core when the discharge interacted too strongly with the CPS [3]. Too much Li ejection into the plasma column was seen to lead to MHD instability and subsequent plasma disruption in FTU [12]. It was also observed that electromagnetic forces led to

* Corresponding author. Tel.: +86 55165591353; fax: +86 55165591310.
E-mail address: hujs@ipp.ac.cn (J.S. Hu).

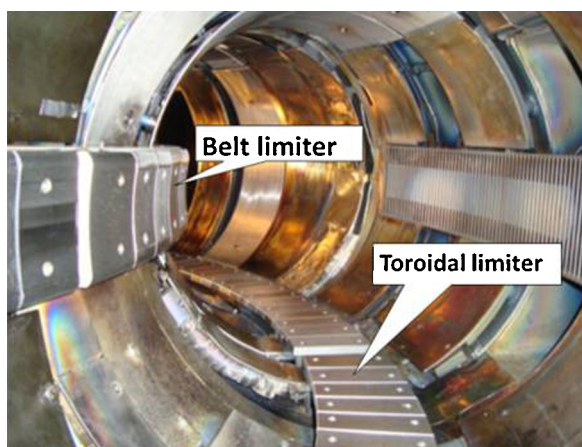


Fig. 1. Inner structures of HT-7.

an uncontrolled ejection of liquid Li from the DIII-D DIMES probe which subsequently caused a major plasma disruption [13,14].

On HT-7 several experiments with different LLLs have been performed since 2009 in order to master the key technologies needed to operate plasmas with liquid limiters so as to improve fusion performance. Some encouraging results were achieved [15,16] during this effort. The results demonstrated that by using a LLL, H recycling was reduced 20–30%, impurity emission decreased about 10–20%, the particle confinement time increased by a factor of 2, and the energy confinement time increased 20%. However, excessive ejection of liquid Li from the LLLs and frequent disruptions also characterized the experiments [17].

The organization of this manuscript is as follows: an overview of the work is presented in Section 1. A description of HT-7 and the experimental arrangement is given in Section 2. The strong interaction between liquid Li and the plasma is documented in Section 3. An analysis of the probable causes of Li efflux including evaporation, sputtering and Li droplet ejection by electromagnetic forces is presented in Section 4. Individual performance analyses of the five types of LLLs tested in this work are presented in Section 5, i.e. the static free-surface and CPS configurations as well as flowing TEMHD and two separate thin film limiters (designated below as the free-surface LLL, CPS LLL, TEMHD FLLL, FLLL(I) and FLLL(II), respectively). Finally the conclusions drawn from the experiments are presented in Section 6.

2. Experimental setup

HT-7 has a major radius (R) of 1.22 m and a minor radius (r) of 0.27 m. Deuterium was the working gas of the plasma discharges. HT-7 employs two toroidal limiters (top and bottom) and one belt limiter for a total limiter surface area of 1.88 m^2 [18]. Before 2011 doped graphite (1% B, 2.5% Si, and 7.5% Ti) with a $\sim 100 \mu\text{m}$ SiC coating was used as the PFM. The limiter material was changed to Mo for the 2011 and 2012 run campaigns. The inner structures of HT-7 with Mo limiters are shown in Fig. 1. The intensity of the lithium emission (LiI at 670.8 nm) was measured by a spectrometer located on the top port of limiter.

Movable LLLs with both static-free-surface and capillary porous system (CPS) configurations were successively utilized in HT-7 during the 2009 and 2011 run campaigns. These limiters were supported by a heated SS tray 3 mm deep and with a plasma-facing area of $\sim 377 \text{ cm}^2$ which was mounted on a movable probe and could thus be positioned at the bottom plasma edge in a controlled fashion from $r = 290 \text{ mm}$ to $r = 260 \text{ mm}$ [16].

A LLL with rudimentary CPS configuration employed two layers of SS meshes with 0.1 mm wire diameters and $0.15 \text{ mm} \times 0.15 \text{ mm}$

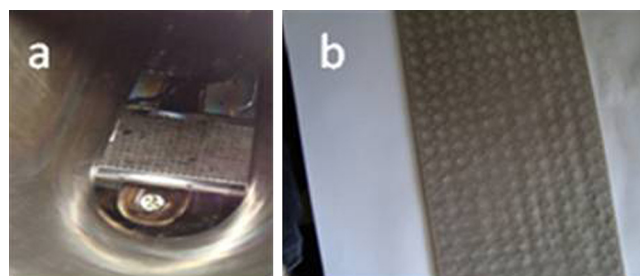


Fig. 2. Photos of LLL with (a) the original CPS configuration with wires and (b) a solid SS plate with many holes.

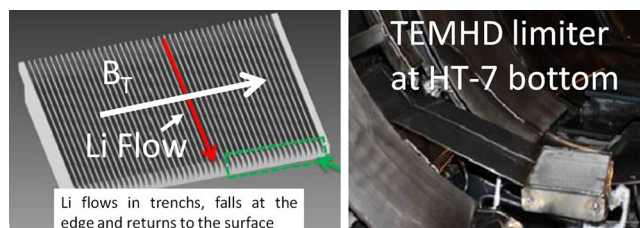


Fig. 3. The TEMHD liquid Li limiter showing the location and orientation of the Li liquid-filled trenches.

open spaces to cover the SS tray with 286 equally spaced apertures [15]. This first attempt at a CPS structure is shown in Fig. 2(a). A second version of a CPS was comprised of a thick solid SS plate with a regular pattern of holes as shown in Fig. 2(b). Before the static LLL experiments, a solid Li plate was placed over the SS tray while the HT-7 vacuum vessel was vented to air and later melted in vacuum. As a practical matter, however, this procedure led to Li surface contamination before the experiment could be carried out. Also, once the Li was exhausted, the LLL experiments had to be terminated. In order to address these problems a CPS with re-filling capability was deployed during the 2011 run campaign. This second version of the CPS had dimensions of $285 \text{ mm} \times 145 \text{ mm} \times 2.5 \text{ mm}$ and pore radii of $\sim 0.1 \text{ mm}$ [17].

In addition to the two static LLLs discussed above, three flowing liquid Li limiters (FLLs) with different free-surface designs were tested in the 2012 campaign [1,19]. One design, developed at the University of Illinois is shown in Fig. 3 [20], and was intended to exploit the thermoelectric magnetohydrodynamic (TEMHD) effect [21]. This system was mounted at the HT-7 bottom on the movable probe described above. The other two FLLs (FLLL(I) and FLLL(II)) employed a thin-film flowing concept [19]. FLLL(I), which was developed at the Chinese Academy of Science Institute of Plasma Physics (ASIPP), was mounted on the high-field-side just below the equatorial mid-plane. FLLL(II), which was developed at the Princeton University Plasma Physics Lab (PPPL), was located at the high-field-side mid-plane just above FLLL(I). The positions of both FLLs are shown in Fig. 4.

The TEMHD design was composed of two parts, i.e. top and bottom trenches. Liquid Li in the top trench that was exposed to plasma heat flux would produce TEMHD current between the liquid Li and SS trench wall due to the thermoelectric effect. The current and device magnetic field would produce a TEMHD force to drive liquid Li along channels. On the top trench, channels were 5 mm in depth and 2 mm in width. It was observed that liquid Li flowed along the trenches at $\sim 42 \text{ mm/s}$ driven by the electromagnetic force, as predicted by theory [22].

In the thin-film FLLL design, liquid Li was driven by argon pressure into a distributor located at the top of a sloped SS guide plate. Liquid Li flowed out from the distributor onto the guide plate where the Li interacted with the edge of the HT-7 plasma column. Finally,

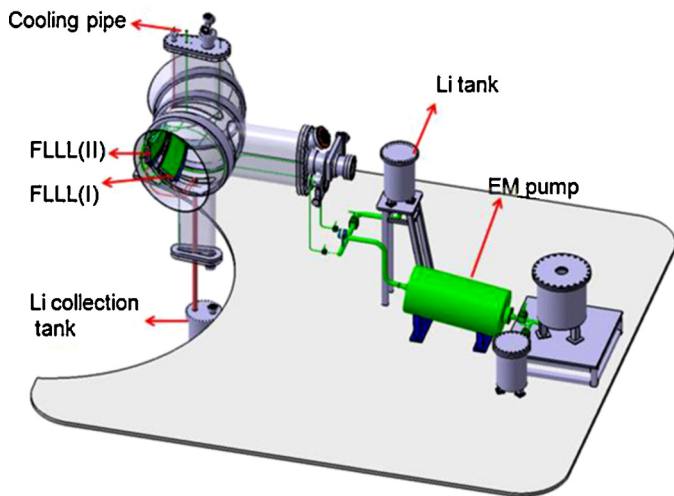


Fig. 4. Shown are the two thin-film FLLs tested in HT-7: FLLL(I) developed at ASIPP and FLLL(II) developed at PPPL. Also seen is the external support hardware needed to service the FLLs.

the Li flowed into collector located at the bottom of the guide plate under the action of gravity. During the experiments it was observed that - when the guide plate was pre-treated with a Li coating before forced Li injection took place - the liquid Li did, in fact, flow slowly and uniformly along the guide plate surface.

3. The strong interaction between liquid Li and the plasma

During the initial experiments with a free-surface LLL a high percentage of the OH discharge attempts resulted in disruptions or in a failure to achieve breakdown when the LLL was located between $r=270$ mm and 260 mm. During this work typical successful discharge durations were 0.4–0.8 s. As shown in Fig. 5, when the LLL surface was located at $r=270$ mm. Li efflux/emission was a serious problem during the plasma current ramp-up and disruption phases of the discharges. During the current ramp-up, Li droplets appeared to be ejected into the plasma edge and strong LiI line emission (670.8 nm) was observed. Subsequently, at the end of current ramping-up, Li emission decreased slightly before finally stabilizing. During the current flat-top phase, Li emission typically remained high with small sawtooth-like fluctuations -

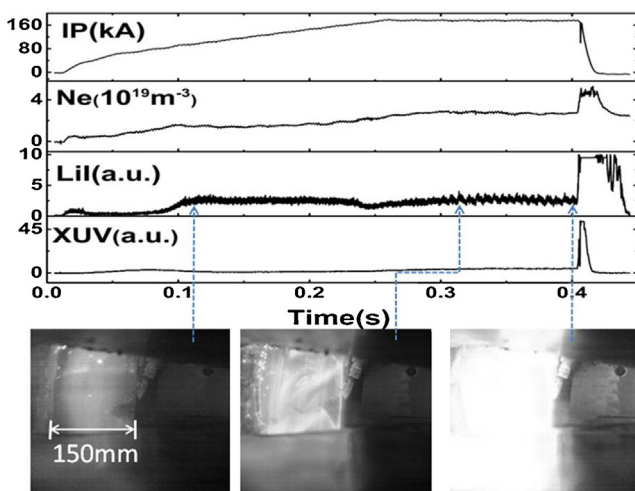


Fig. 5. Shown are images of the free-surface LLL located at the bottom of HT-7 (image rotated) showing Li effluxes at different phases of the discharge and the corresponding plasma parameters.

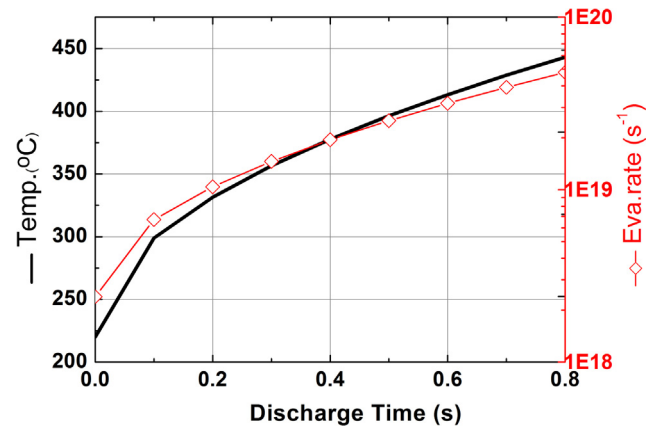


Fig. 6. Predicted Li surface temperature and evaporation rates during a typical OH discharge.

probably due to plasma instabilities. Immediately before disruptions, it was noted that Li line emission grew abruptly as did the plasma density and extreme ultraviolet (XUV) emission. After the plasma disruption LiI line emission typically saturated for ~ 0.04 s. These observations indicated that a strong interaction between the Li and the plasma took place when the discharge was run on the free-surface LLL. Enhanced Li emission from the LLL was associated with plasma instability and disruptions, and those disruptions led to more Li emission from the LLL.

4. Probable causes of Li efflux

In order to reduce Li efflux from LLLs and thus suppress plasma disruptions, several likely causes of the efflux were analyzed including evaporation, sputtering and Li droplet ejection.

4.1. Li evaporation

So as to understand the role of Li evaporation, the HT-7 limiter surface temperature was estimated as follows [13,23]:

$$T = T_0 + 2q \left(\frac{t}{\pi \rho c k} \right)^{1/2} \quad (1)$$

where T_0 is the initial limiter temperature (in $^{\circ}\text{C}$), q is the heat flux from the plasma (MW/m^2); t is the plasma pulse length (s); ρ is the limiter material density (kg/m^3); c is the average limiter specific heat capacity ($\text{J}/\text{kg K}$) and k is the limiter thermal conductivity ($\text{W}/\text{m K}$).

On HT-7, discharges typically had OH input power of ~ 200 kW. When the LLL was located at $r=260$ mm, half of the plasma power was assumed to be incident onto the LLL surface with initial temperature of ~ 220 $^{\circ}\text{C}$ [24]. Modeling results of the LLL surface temperature and evaporation rate as functions of time during the discharge are shown in Fig. 6. It may be noted that - in this estimate - the maximum LLL surface temperature increased to ~ 443 $^{\circ}\text{C}$ at $t \sim 0.8$ s and the calculated evaporation rate of Li atoms was $< 4 \times 10^{19} \text{ s}^{-1}$.

In order to evaluate Li evaporation from an LLL experimentally, a non-disruptive OH discharge was run against an unheated limiter tray filled with solid Li. During the discharge the Li surface temperature was measured by infrared (IR) camera located on the top port of HT-7 and by embedded thermocouples (TC), which were inserted into several positions on the SS tray within 1 mm of the Li surface. Previous calibration found that thermal-radiative emissivity of solid lithium is about 0.3. The temporal evolutions of discharge parameters during of shot 106,024 ($I_p = 120$ kA, $n_e = 1.4 \times 10^{19} \text{ m}^{-3}$,

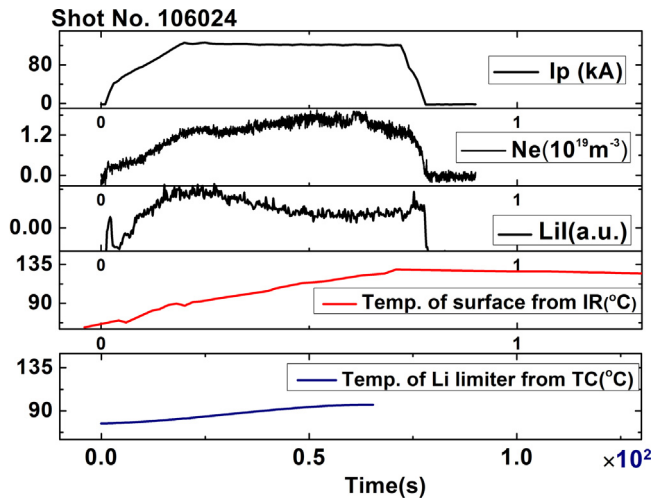


Fig. 7. Basic discharge parameters of a typical OH discharge run against a solid Li limiter with embedded thermocouples and monitored with an IR camera.

and duration = 0.78 s) which was run against the solid Li limiter located at $r = 260$ mm are shown in Fig. 7.

As can be seen, the Lil line emission was strong during current ramp-up before reaching a lower but relatively stable level. It can be noted from the IR and TC measurements that the maximum surface temperature of Li limiter increased less than 70°C during the discharge. This indicated that the increase of Li surface temperature was less than the estimated value (from above). This disparity is probably due to the rough calculation method employed in estimating the surface temperature of the Li limiter and a larger assumed heat flux than was warranted. Based on both the modeling results and the measurements described above, however, it can be concluded that – for the HT-7 OH discharges lasting 0.8 s employed in this work – Li evaporation was negligible compared to other Li efflux processes.

4.2. Li sputtering

When a LLL was employed, Li was sputtered by both incident Li and D particles. The particle influx per area onto the LLL surface can be represented by [13,25]:

$$\Gamma_i = \frac{1}{2} n_e C_s \sin \theta \quad (2)$$

where n_e is the plasma density, C_s is the ion particle speed and θ is the angle of the magnetic field line with respect to the LLL surface. Typically, during the HT-7 LLL discharges studied in this

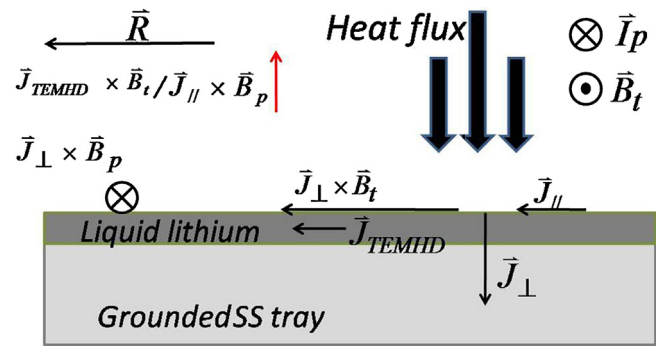


Fig. 8. Basic forces acting on free standing liquid Li.

work, $n_e = 2 \times 10^{19} \text{ m}^{-3}$, the edge electron temperature $T_e = 40 \text{ eV}$ as measured by a Langmuir probe, and the angle of magnetic field line with respect to the LLL surface was $\theta \sim (0-2)^\circ$. Drawing on the sputtering results from T-11M, when the liquid Li temperature is less than 500°C , the measured sputtering coefficient is expected to be 0.5–1 [11]. Assuming this coefficient and calculating the influx rate per area from Eq. (2), the Li sputtering atomic efflux into the plasma from the area of the LLL is expected to be $<(1-2) \times 10^{20}/\text{s}$.

4.3. Ejection of Li droplets

As monitored by a fast camera, many liquid droplets with radii $\sim 0.5-5 \text{ mm}$ were ejected from the LLLs during the discharges studied in this work. As shown in Fig. 5 many Li droplets with radius $\sim 0.8 \text{ mm}$ were ejected into plasma edge and were subsequently ablated. A single droplet of similar size would bring $\sim 1.0 \times 10^{20}$ Li particles into the plasma. Because many Li droplets were ejected in typical disruptive discharges lasting $<0.8 \text{ s}$, it may be concluded that the efflux rate resulting from Li ejection was clearly much larger than that from either Li evaporation or sputtering – each independently estimated above as $<10^{20} \text{ atoms/s}$. Hence, the ejection of Li droplets was the main cause of plasma disruptions in this work.

In order to investigate the causes of Li droplet ejection, the forces acting on static-surface liquid Li during HT-7 discharges were analyzed in detail. In the HT-7 LLL geometry the direction of gravity was obviously downward and tended to keep the liquid Li in the SS tray. The surface tension of liquid Li also acted to prevent ejection of liquid Li from the SS tray. The plasma flow and basic electromagnetic forces are described in Fig. 8. During the LLL campaign the plasma current direction was clockwise and toroidal magnetic field direction was counterclockwise. Plasma flow was in the same direction as the plasma current. The LLL was grounded and the total current in the liquid Li from the SOL current and induced current

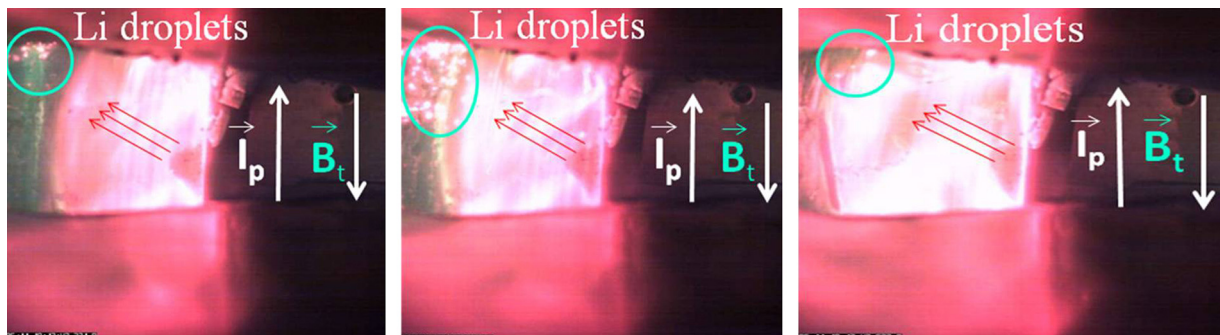


Fig. 9. Liquid Li movement in and droplet ejection from the LLL located at the bottom of HT-7 (image rotated).

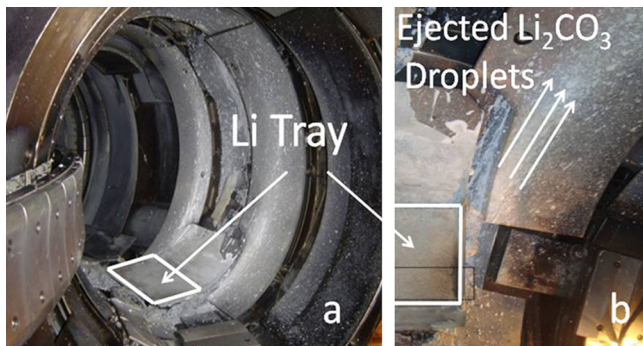


Fig. 10. Deposited spots of Li/Li₂CO₃ on the walls of the vacuum vessel seen near the LLL after exposure to air.

had two components: one straight down (J_{\perp}) and the other parallel to the LLL surface (J_{\parallel}). The total current produced a net force with components: $J_{\perp} \times B_p$ (in the same direction as the plasma current), $J_{\perp} \times B_t$ (along the major radius), and $J_{\parallel} \times B_p$ (the vertical force tending to eject droplets toward the plasma core). In addition, due to the temperature gradient parallel to the face of the Li, a TEMHD force would be produced that added to the $J_{\parallel} \times B_p$ force pointing to the plasma core R .

Because the liquid Li in the tray could be expected to move in the direction of the net electromagnetic force, it was anticipated that the direction of ejected droplets would have both toroidal and poloidal components. As seen in Fig. 9, it was observed that, during HT-7 discharges, liquid Li flowed along the direction between the radial and toroidal directions, and liquid Li droplets were preferentially ejected from the top left corner in a direction which was consistent with analysis given above.

After completion of the experiments, the HT-7 vacuum vessel was exposed to air. Li deposited on the vessel walls was thus quickly transformed into Li₂CO₃ – a stable white compound. It was subsequently observed that most of the white Li₂CO₃ areas were distributed in a range of ~ 1 m around the LLL, as shown in Fig. 10. It may be seen that the density of Li₂CO₃ “droplet spots” gradually decrease along a direction with both toroidal and poloidal components. This observation is considered as reinforcement of the ideas and analysis of the electromagnetic forces discussed above.

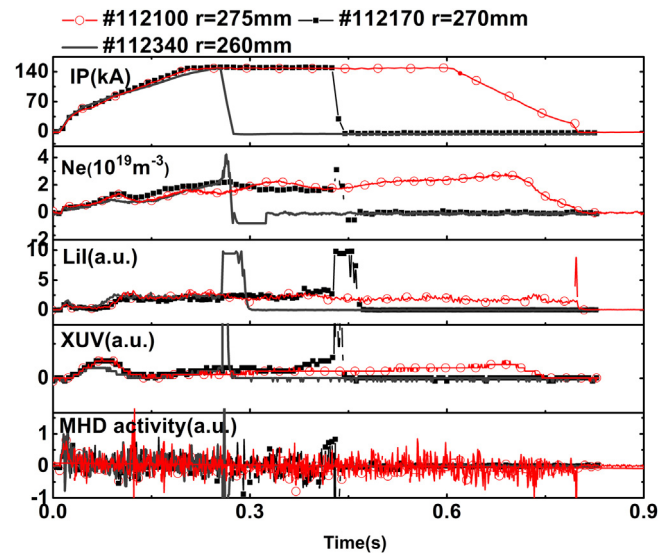


Fig. 11. Comparison of three plasmas run on a free-surface LLL as the radial position of the limiter was changed.

5. Li efflux from different Li surfaces

5.1. Li efflux from static LLLs

5.1.1. Comparison of Li efflux and plasma behavior at different LLL positions

In order to investigate the plasma-LLL interaction, several discharges with similar currents and densities were run against the movable free-standing LLL located at each of three radial positions. Generally, these discharges could be characterized in two ways: either as normal (i.e. proceeding for 0.8 s) or as disruptive (i.e. ending in a major disruption well before 0.8 s). It was observed that the clear majority of discharges proceeded normally when the LLL was positioned at $r=275$ mm; that $\sim 2/3$ plasmas were disruptive with the LLL at $r=270$ mm; and that $\sim 9/10$ plasmas were disruptive with the LLL at $r=260$ mm. This clear statistical trend in disruptive behavior as the limiter was moved inward toward the plasma edge indicates an increasingly stronger interaction of the plasma with the liquid Li. During these experiments it was further observed that the effective duration of the discharges was strongly related to the

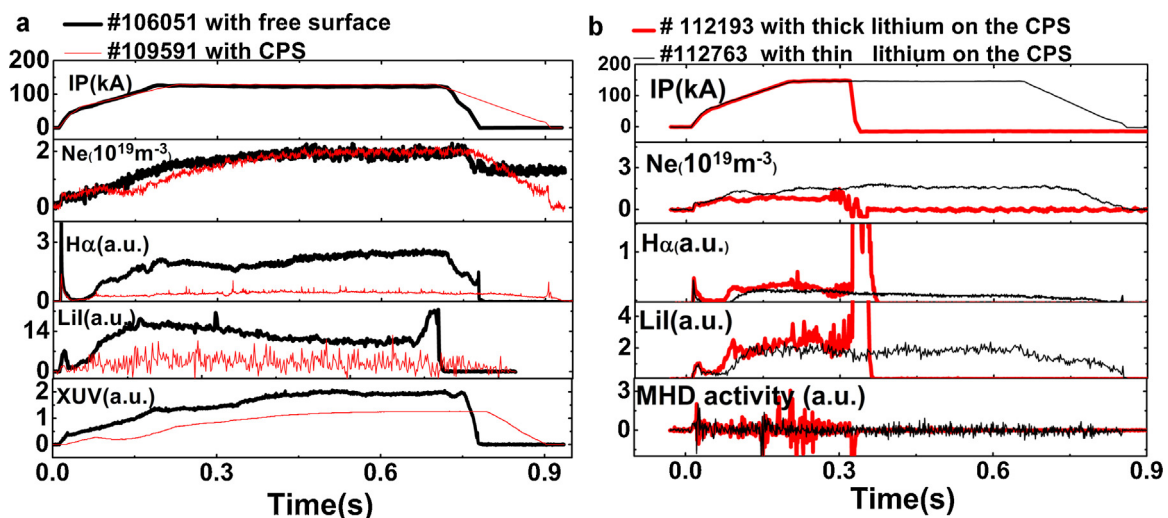


Fig. 12. Comparison of plasma discharges with different situations, (a) between free surface and CPS, (b) between thick and thin Li on the CPS.

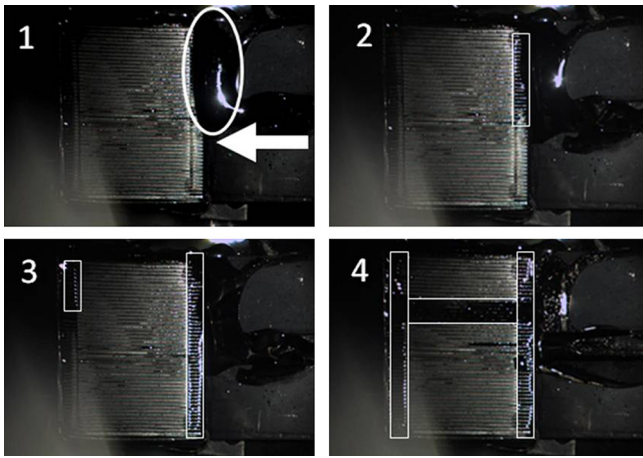


Fig. 13. Time-lapse photographs of liquid Li injection into the TEMHD FLLL. The boxes drawn on the figures show which parts of the structure have Li all the way to the surface. Even in frame 4, most of the surface does not have lithium present.

LLL radial position. The average duration of these discharges clearly decreased as the LLL was positioned closer to the plasma edge. Typical examples of these discharges are shown in Fig. 11. Shots 112,100, 112,170 and 112,340 were run with the LLL positioned at $r = 275$ mm, 270 mm and 260 mm, respectively.

5.1.2. Comparison of Li efflux and plasma behavior between static-free-surface and CPS LLLs

As shown in Fig. 12(a), two plasmas with similar Li temperatures of $\sim 230^\circ\text{C}$ were compared. Shots 106,051 and 109,591 employed free-surface and CPS LLLs, respectively. It may be noted that plasma with a free-surface LLL had stronger $\text{H}\alpha/\text{LiI}$ line emissions and higher XUV radiation.

Shots 112,193 and 112,763 were run on a CPS LLL which had thick and thin liquid Li films, respectively. The initial thickness of the Li layer was determined by the amount of Li injected onto the CPS before the experiment. After running several shots, $\sim 4/5$

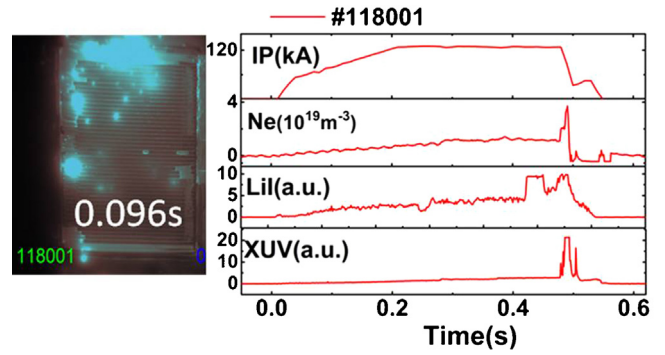


Fig. 14. Liquid Li ejection from the TEMHD FLLL and a subsequent plasma disruption.

amount of Li on the surface of CPS was consumed, so the initial Li layer became thin. During these CPS experiments it was observed that plasmas run against a thick Li surface were disruptive and exhibited higher LiI/Ne and $\text{H}\alpha/\text{Ne}$ levels. Subsequent plasmas run against the CPS with a thin Li layer proceeded normally.

Further, from the study of many photographs [17], it was observed that – when employing the CPS LLL – the number and size of Li droplets deposited on the vacuum vessel wall were reduced as compared to the those resulting from the use of a free-surface LLL. These observations are consistent with the general result that use of the CPS LLL resulted in lower recycling, lower impurity influx and milder disruptions as compared to the use of the free-surface LLL.

5.2. Li efflux from FLLs

5.2.1. Li efflux and plasma behavior with a TEMHD FLLL

As mentioned above, in 2012, two main designs of flowing liquid Li limiters (FLLL) were tested. One design attempted to exploit TEMHD forces as shown in Fig. 3 and the other two involved a thin-film flowing concept as shown in Fig. 4 above.

During the initial attempt to inject liquid Li onto the TEMHD FLLL it was generally difficult to fill the channel trenches. This poor

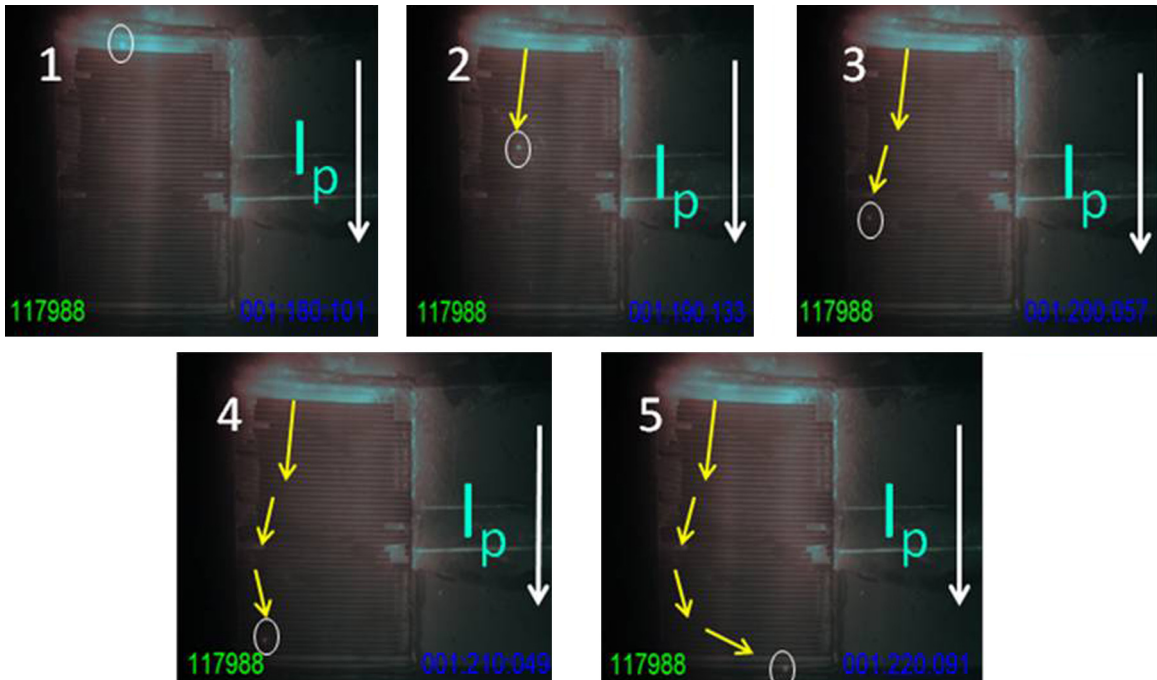


Fig. 15. The movement of a single liquid Li droplet captured fortuitously as it leaves the TEMHD FLLL and enters the plasma.

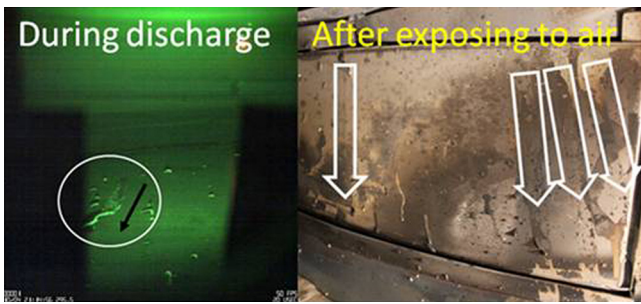


Fig. 16. Non-uniform Li flow along the SS plate of FLLL(I) was apparent during plasma operation and was consistent with the Li remnants found after exposure to air (images rotated).

wetting was possibly due to unclean SS channel surfaces and surface temperatures which were lower than the bulk temperature. In addition not enough Li was added to the structure. In any case, as shown in Fig. 13, only a few of the channels appeared to have wetted and filled as planned.

During discharges using the TEMHD FLLL, liquid Li was observed to flow along the trenches at ~ 42 mm/s driven by the electromagnetic force [1]. However, it was also observed that liquid Li droplets of various sizes were ejected from the limiter during discharges and led to plasma disruptions, as shown in Fig. 14. The probable cause of this ejection was the observed incomplete fill of liquid Li to the SS channels. This problem led to reduced contact between the liquid Li and SS surfaces. The poor wetting is thought to have facilitated the ejection of Li droplets from the limiter during discharges due to electromagnetic forces. Complete filling would likely prevent such ejection.

As shown in Fig. 15, the movement of a single liquid Li droplet emitted from the TEMHD FLLL was captured. The direction of plasma current is marked in the images. A liquid Li droplet is emitted from one side of the FLLL, and initially moves along the direction of the yellow arrows to the other side. It was clearly observed that the Li droplet initial movement was along the direction of plasma current with a velocity of 4 m/s and formed a curved trajectory. This suggests that when the Li droplet entered the plasma, the droplet surface quickly became charged and so moved under the influence of the magnetic field to cause a curved movement.

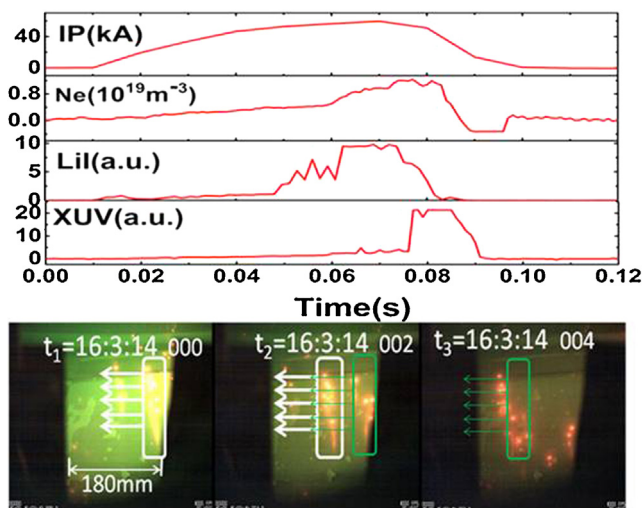


Fig. 17. Plasma performance and Li droplet movement with non-uniform Li flow. Over the 4 ms duration shown above, ejected droplets are captured moving at 20–100 m/s.

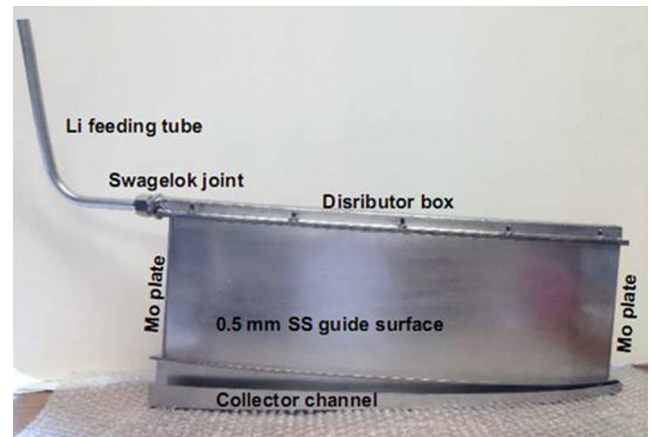


Fig. 18. Shown is the plasma facing surface of FLLL(II). During plasma operation, a thin wetted film of liquid Li flowed through holes spaced 0.8 mm apart in the manifold at the top to a collector channel at the bottom and eventually to an external Li storage tank (see Fig. 4).

5.2.2. Li ejection and plasma behavior with thin flowing film LLLs

Two versions of a FLLL which employed the concept of a thin flowing Li film were tested in HT-7. The first version (FLLL(I) in Fig. 4) was not treated with a Li coating before Li injection began. As shown in Fig. 16, extremely non-uniform flow of Li along the limiter plate was observed during plasma discharges which indicated poor wetting of Li to the SS plate. Using FLLL(I), plasma breakdown was difficult to achieve and most discharges ended in disruptions owing to Li droplet ejection. The Li droplets were observed to move along the direction of plasma current with velocities of ~ 20 –100 m/s, as shown in Fig. 17.

The other version of a thin-film limiter (FLLL(II) in Fig. 4 and shown in detail in Fig. 18) was pre-treated with a Li coating applied before injection of flowing Li. It was subsequently observed that a thin film of Li which flowed along the SS plate could be obtained during plasma discharges when employing this pre-treatment.

Most discharges run against FLLL(II) proceeded normally with only infrequent ejections of small Li droplets and without disruptions. This was in marked contrast to those discharges run against FLLL(I) with non-uniform flow and frequent ejections of large Li droplets which often caused disruptions. The improved

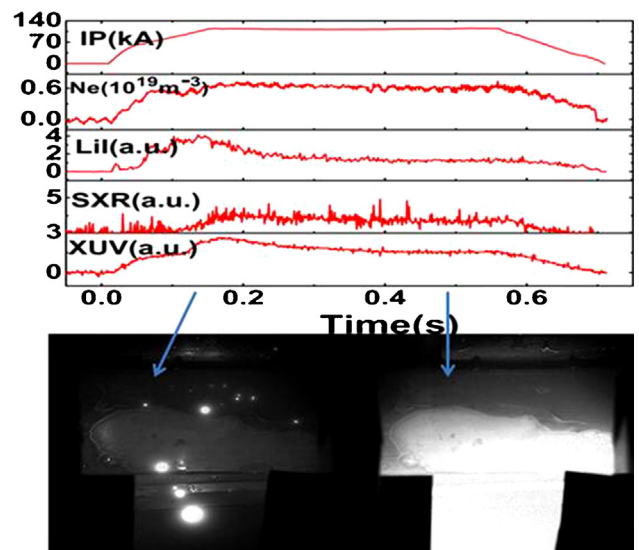


Fig. 19. Liquid Li behavior and plasma performance with thin and uniform Li flow exhibited with FLLL(II).

performance of FLLL(II) was likely due to the good wetting of the uniform Li film brought about by Li pre-coating. It appears that the strong adhesion associated with improved wetting was capable of resisting the HT-7 electromagnetic forces and thus prevented Li ejection as demonstrated in Fig. 19.

6. Conclusions

Successful experiments with both static and flowing LLLs have been performed in HT-7 since 2009. The experiments were undertaken in order to understand the causes and consequences of ejected Li as well as to investigate the effects of surface structures on the ejection process.

During this work it was observed that strong Li droplet ejection mainly due to $J \times B$ force generally led to disruptive plasmas when using a static free-surface LLL. As compared to a free surface structure, the CPS surface suppressed the ejection of Li droplets and proved to be a benefit for plasma operation.

Further, the ejection of Li from a TEMHD FLLL and from two versions of thin-film FLLLs was compared. Possibly due to incomplete filling and poor initial wetting of the associated trench structures, strong ejection of Li was observed from the TEMHD FLLL.

It was observed that the ejection of Li was significantly reduced when the plasma was run against the pre-treated thin-film FLLL(II) as compared to any of the limiters tested in this work. In addition the liquid Li was seen to flow slowly and uniformly when the FLLL(II) flow plate (seen in Fig. 18) was pre-treated with an evaporative Li coating to promote improved Li wetting. The resulting performance of the associated plasma was clearly improved.

In EAST, designs for accommodating a W divertor as well as a movable outboard FLLL are under development. Li surface control should be improved by enhancement of surface wettability and the proper choice of limiter surface structure. By employing the CPS configuration or a thin Li layer for a FLLL, liquid Li should be effectively confined. Further, during future EAST discharges with high input power and long pulse duration, an actively cooled system should be available to prevent elevated Li evaporation due to the high surface temperature of FLLLs.

Acknowledgements

The authors thank D.K. Mansfield for fruitful discussions and English correction for this paper. This research was funded by National Magnetic Confinement Fusion Science Program

under Contract No. 2013GB114004 No. 2013GB107000 and No. 2011GB10700, National Nature Science Foundation of China under Contracts No. 11075185 and No. 11021565, and the JSPS-NRF-NSFC A3 Foresight Program in the field of Plasma Physics (NSFC No. 11261140328).

References

- [1] J. Ren, J.S. Hu, G.Z. Zuo, Z. Sun, J.G. Li, D.N. Ruzic, et al., *Phys. Scr.* T159 (2014) 014033 (5pp).
- [2] T.D. Rognlien, M.E. Rensink, *J. Nucl. Mater.* 290–293 (2001) 312.
- [3] G.Y. Antar, R.P. Doerner, R. Kaita, R. Majeski, J. Spaleta, T. Munsat, et al., *Fusion Eng. Des.* 60 (2002) 157.
- [4] R. Kaita, P. Efthimion, D. Hoffman, B. Jones, H. Kugel, R. Majeski, et al., *Rev. Sci. Instrum.* 72 (2001) 915.
- [5] R. Majeski, S. Jardin, R. Kaita, T. Gray, P. Marfuta, J. Spaleta, et al., *Nucl. Fusion* 45 (2005) 519.
- [6] R. Kaita, R. Majeski, M. Boaz, P. Efthimion, G. Gettelfinger, T. Gray, et al., *J. Nucl. Mater.* 337–339 (2005) 872.
- [7] G. Mazzitelli, M.L. Apicella, V.P. Ridolfini, G. Apruzzese, R. De Angelis, D. Frigione, et al., *Fusion Eng. Des.* 85 (2010) 896.
- [8] M. Apicella, G. Mazzitelli, V. Lazarev, E. Azizov, S. Mirnov, V. Petrov, et al., *Fusion Eng. Des.* 75–79 (2005) 351.
- [9] V. Pericoli-Ridolfini, A. Alekseyev, B. Angelini, S.V. Annibaldi, M.L. Apicella, G. Apruzzese, et al., *Nucl. Fusion* 47 (2007) S608.
- [10] S.V. Mirnov, V.B. Lazarev, S.M. Sotnikov, V.A. Evtikhin, I.E. Lyublinski, A.V. Vertkov, et al., *Fusion Eng. Des.* 65 (2003) 455.
- [11] S.V. Mirnov, E.A. Azizov, V.A. Evtikhin, V.B. Lazarev, I.E. Lyublinski, A.V. Vertkov, et al., *Plasma Phys. Control. Fusion* 48 (2006) 821.
- [12] M.L. Apicella, G. Apruzzese, G. Mazzitelli, V.P. Ridolfini, A.G. Alekseyev, V.B. Lazarev, et al., *Plasma Phys. Control. Fusion* 53 (2012) 035001 (10 pp).
- [13] J.P. Allain, D.G. Whyte, J.N. Brooks, *Nucl. Fusion* 44 (2004) 655.
- [14] D. Whyte, T. Evans, C. Wong, W. West, R. Bastasz, J. Allain, et al., *Fusion Eng. Des.* 72 (2004) 133.
- [15] G.Z. Zuo, J.S. Hu, J.G. Li, N.C. Luo, L.E. Zakharov, L. Zhang, et al., *J. Nucl. Mater.* 415 (2011) S1062.
- [16] J.S. Hu, G.Z. Zuo, J.G. Li, N.C. Luo, L.E. Zakharov, L. Zhang, et al., *Fusion Eng. Des.* 85 (2010) 930.
- [17] Z. Sun, J.S. Hu, G.Z. Zuo, J. Ren, J.G. Li, L.E. Zakharov, et al., *J. Nucl. Mater.* 438 (2013) S899.
- [18] J.S. Hu, J.G. Li, X.M. Wang, H.T. team, *Plasma Phys. Control. Fusion* 47 (2005) 1271.
- [19] J.S. Hu, J. Ren, Z. Sun, G.Z. Zuo, Q.X. Yang, H.L. Bi, et al., *New progresses of Li applications on HT-7 and EAST in 2012*, in: 3rd International Symposium on Lithium Applications for Fusion Devices, Frascati, Italy, 2013.
- [20] D.N. Ruzic, W. Xu, D. Andruczyk, M.A. Jaworski, *Nucl. Fusion* 51 (2011) 102002 (4pp).
- [21] M.A. Jaworski, T.K. Gray, M. Antonelli, J.J. Kim, C.Y. Lau, M.B. Lee, et al., *Phys. Rev. Lett.* 104 (2010) 094503.
- [22] W. Xu, D. Curreli, D. Andruczyk, T. Mui, R. Switts, D.N. Ruzic, *J. Nucl. Mater.* 438 (2013) S422.
- [23] H. Chen, Q. Li, G.N. Luo, H.Y. Guo, *Fusion Eng. Des.* 85 (2010) 2111.
- [24] S. Carpentier, Y. Corre, M. Chantant, R. Daviot, G. Dunand, J.L. Gardarein, et al., *J. Nucl. Mater.* 390–391 (2009) 955.
- [25] P.C. Stangeby, C.S. Pitcher, J.D. Elder, *Nucl. Fusion* 32 (1992) 2079.